Computer-generated holograms of three-dimensional realistic objects recorded without wave interference

Youzhi Li, David Abookasis, and Joseph Rosen

We propose a method of synthesizing computer-generated holograms of real-life three-dimensional (3-D) objects. An ordinary digital camera illuminated by incoherent white light records several projections of the 3-D object from different points of view. The recorded data are numerically processed to yield a two-dimensional complex function, which is then encoded as a computer-generated hologram. When this hologram is illuminated by a plane wave, a 3-D real image of the object is reconstructed. © 2001 Optical Society of America

OCIS codes: 090.1760, 070.2580, 070.4560, 100.6890.

1. Introduction

Since the invention of the hologram more than 50 years ago,[1] holographic recording of real objects has been performed by wave interference. In general, interference between optical waves demands special stability of the optical system and relatively intense light with a high degree of coherence between the involved beams. These requirements have prevented hologram recorders from becoming as widely used for outdoor photography as conventional cameras. A partial solution to these limitations is obtained by the techniques of holographic stereograms[2,3] (also known as multiplex holograms[4,5]). However, optical interference is also involved in recording of holographic stereograms, although it is off-line interference. The meaning of "off-line" here is that a reference beam interferes with a beam diffracted from a motion picture film. The motion picture film contains many viewpoints of the object, and the object is in-line recorded by a motion picture camera. However, unlike ordinary holograms,[1,6] holographic stereograms do not reconstruct the true wave front that is diffracted from an object when this object is coherently illuminated. The reconstructed wave front from a holographic stereogram is composed of a set of discrete patches; each patch contains a different perspective projection of the object. Because of the discontinuity between those patches, the imitation of the observed reality cannot be complete.

In this study we propose a process of recording a computer-generated hologram (CGH) of a real-world three-dimensional (3-D) object under conditions of incoherent white illumination. Yet the true wave front diffracted from the object, when it is coherently illuminated, can be reconstructed from the proposed hologram. In other words, after a process of recording the scene under incoherent illumination and digital computing, we get a two-dimensional (2-D) complex function. This function is equal to the complex amplitude of coherent light diffracted from the same object and propagates through a particular optical system described below. Thus apparently we succeed in recording the complex amplitude of some wave front without beam interference. It should immediately be said that we do not propose here a general method of recording complex amplitude without interference. Our system cannot sense any phase modulations that happen between the object and the recording system. However, let us look at a 3-D object illuminated by a coherent plane wave. If the reflected beam from the object propagates in free space and then through the particular optical system, the result at the output plane is some complex amplitude. We claim that this complex amplitude can be restored under incoherent conditions. Once this complex function is in computer memory, we can encode it to a CGH. When this CGH is illuminated by a plane wave, which then propagates through the same optical system mentioned above, the image of

Y. Li, D. Abookasis, and J. Rosen (rosen@ee.bgu.ac.il) are with the Department of Electrical and Computer Engineering, Ben-Gurion University of the Negev, P.O. Box 653, Beer-Sheva 84105, Israel.

Received 25 September 2000; revised manuscript received 27 February 2001.

0003-6935/01/172864-07$15.00/0

© 2001 Optical Society of America

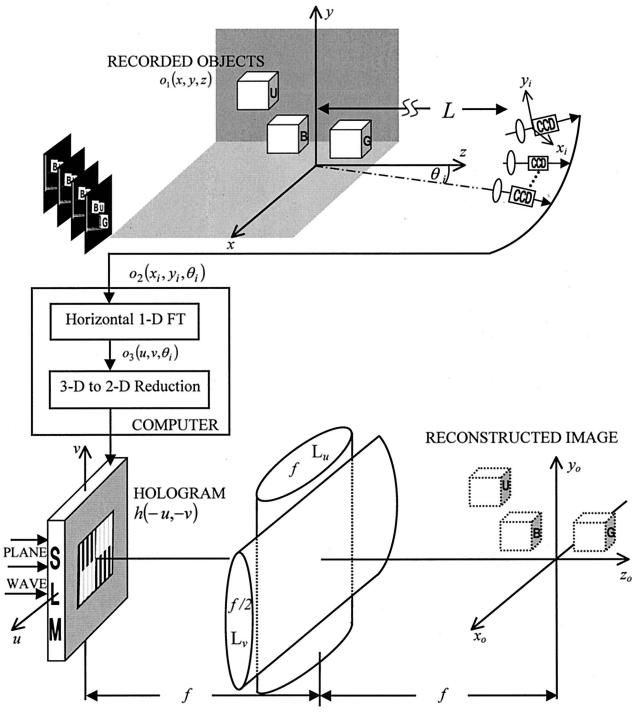

Fig. 1. Schematic of the holographic recording and reconstructing systems. SLM, spatial light modulator.

the 3-D object is reconstructed in space as a common holographic image.

Similarly as in stereogram photography, we record several digital pictures of the object from different points of view. The pictures are recorded into a digital computer, which computes a CGH from the input data. Illuminating this hologram by a plane wave reconstructs the original objects and creates the volume effect in the observer's eyes. The hologram that we would like to produce is of the type of a Fourier hologram. This means that the image is reconstructed in the vicinity of the back focal plane of a spherical lens when the hologram is displayed on the front focal plane. However, a complete 2-D Fourier hologram can be recorded if the camera's points of view are on a 2-D transverse grid of points. Because it is technically impractical, or at least quite difficult, to shift the camera out of the horizontal plane along a 2-D transverse grid of points, the hologram that we produce here is only a one-dimensional (1-D) Fourier hologram along the horizontal axis and an image hologram along the vertical axis. Consequently, the coherent system that we emulate and the reconstructing system are both composed of a cylindrical Fourier lens in the horizontal axis and a second cylindrical imaging lens in the vertical axis. In Section 2 we describe the recording process in detail.

2. Recording and Synthesizing the Computer-Generated Hologram

The recording setup is shown in the upper part of Fig. 1. A 3-D object function $o_1(x, y, z)$ is located at the coordinate system (x, y, z). $o_1(x, y, z)$ represents the intensity reflected from all the observed bodies in the scene. From each point of view, the camera observes the scene through an imaging lens located at a distance L from the origin of (x, y, z). The camera is actually shifted in constant angular steps along a horizontal arc centered about the origin, and it is always directed to the origin. The angle between the camera's optical axis and the z axis is denoted θ_i. For each θ_i, the projected image $o_2(x_i, y_i, \theta_i)$ is recorded into the computer, where (x_i, y_i) are the coordinates of the image plane of each camera. On the basis of simple geometrical considerations, the relation between (x_i, y_i, θ_i) and (x, y, z) is given by

$$(x_i, y_i) = (x \cos \theta_i + z \sin \theta_i, y). \quad (1)$$

For simplicity, we assume that the magnification factor of the imaging lens is 1. Also, because distance L is much greater than the depth of the object, all the object points are equally imaged with the same magnification factor of 1.

Inside the computer, each projected function is Fourier transformed along horizontal axis x_i only and is imaged along vertical axis y_i. We assume that the digital 1-D Fourier transform (FT) is a perfect imitation of an optical system, such that the collection of 1-D FTs is given by

$$o_3(u, v, \theta_i) \propto \int\int o_2(x_i, y_i, \theta_i)\exp(-i2\pi u x_i/\lambda f) \times \delta(v - y_i)\mathrm{d}x_i\mathrm{d}y_i, \quad (2)$$

where λ is the wavelength of the plane wave illuminating the system and f is the focal length of the cylindrical Fourier lens. The coherent optical system that yields the same result as relation (2) is shown in Fig. 2(a). For each θ_i value, the real positive transparency function $o_2(x_i, y_i, \theta_i)$ is displayed on the front focal plane of lens L_x and then illuminated by a plane wave. Because of the focal length of lens L_y, there is an imaging relation between axes y_i and v. Assuming an ideal system, this image is expressed by the convolution of the object function with a δ function[7] in relation (2). This lens setup is also used later for reconstructing the hologram. Note that the optical system shown in Fig. 2(a) is only the optical equivalent system of the digital computation. The operation expressed in relation (2) is performed by the digital computer to preserve the phase information of the FT of the projections without the use of light interference. The optical equivalent system is presented in Fig. 2(a) for clarity only, not as a system that was really implemented in this study. It should be also emphasized that, although no phase information is contained in any of the object's projections, the phase information that describes the object's 3-D structure is actually recovered by the digital process, as discussed next.

Let us consider now the relation between $o_3(u, v, \theta_i)$ and the object $o_1(x, y, z)$. For a single infinitesimal element of size $(\Delta x, \Delta y, \Delta z)$, at point (x', y', z'), with the intensity $o_1(x', y', z')$ from the entire 3-D object

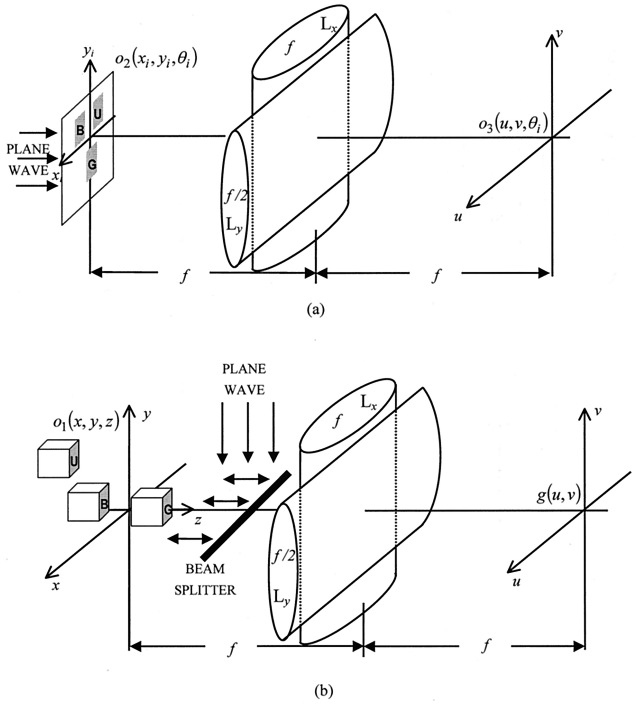

Fig. 2. Equivalent optical systems for (a) the digital computation performed on each projection and (b) the hologram recording.

function, the distribution on the (u,v) plane for each θ_i value is

$$o_3(u, v, \theta_i) \propto o_1(x', y', z')\exp(-i2\pi u x_i/\lambda f) \times \delta(v - y_i)\Delta x\Delta y\Delta z. \quad (3)$$

Relation (3) is obtained from relation (2) because, for each θ_i value, a single point at the input scene is imaged to a point at the (x_i, y_i) plane. The δ function in relation (3) is a mathematical idealization of the fact that the point at y_i is imaged to the line $v = y_i$ on the (u, v) plane. Substituting Eq. (1) into relation (3) yields

$$o_3(u, v, \theta_i) \propto o_1(x', y', z')\exp[-i2\pi(ux' \cos\theta_i + uz' \sin\theta_i)/\lambda f]\delta(v - y')\Delta x\Delta y\Delta z. \quad (4)$$

Next we examine the influence of all points of the object $o_1(x, y, z)$ on the distribution of $o_3(u, v, \theta_i)$. The object is 3-D, and the FT operates only along the horizontal axis, whereas along the vertical axis the picture is perfectly imaged. Therefore the overall distribution of $o_3(u, v, \theta_i)$ is obtained by a 3-D integral of the expression in relation (4) as follows:

$$o_3(u, v, \theta_i) \propto \int\int\int o_1(x, y, z)\exp[-i2\pi(ux \cos\theta_i + uz \sin\theta_i)/\lambda f]\delta(v - y)\mathrm{d}x\mathrm{d}y\mathrm{d}z. \quad (5)$$

Relation (5) describes a tomographic process in the visible-light regime.[8,9] By an appropriate Fourier transform from the spatial frequency coordinates[10] $(f_x, f_z) = (u \cos\theta_i, u \sin\theta_i)$ to (x, z), the 3-D object $o_1(x, y, z)$ can be digitally reconstructed from $o_3(u, v, \theta_i)$ inside the computer. However, it is not our intention here to deal with tomography or with digital reconstruction. Our goal is to pull out from the entire 3-D distribution given in relation (5) a particular 2-D distribution only. This 2-D distribution, when it is encoded into a CGH and illuminated properly, yields a holographic reconstruction of the object.

The maximum range of angle θ_i is chosen to be small (no more than 16° on each side in the present example). Therefore we are allowed to use the following small-angle approximations: $\cos\theta_i \approx 1$ and $\sin\theta_i \approx \theta_i$. Recalling our original goal to get a 2-D hologram containing the information on the objects' volume, we next reduce the 3-D function given by relation (5) to a 2-D function. From the 3-D function $o_3(u, v, \theta_i)$, we take only the 2-D data that exist on the mathematical plane defined by the equation $\theta_i = au$ in the (u, v, θ_i) space, where a is some chosen parameter. Substituting this condition with the small-angle approximations into relation (5) yields the following 2-D function:

$$h(u, v) = o_3(u, v, \theta_i = au)\Big|_{\substack{\cos\theta_i=1 \\ \sin\theta_i=\theta_i=au}} = \int\int\int o_1(x, y, z)\delta(v - y)\exp[-i2\pi(ux + au^2z)/\lambda f]\mathrm{d}x\mathrm{d}y\mathrm{d}z. \quad (6)$$

Let us summarize the process up to this point: The 3-D object $o_1(x, y, z)$ is recorded from several angle values θ_i. In the computer the recorded data of projections of the scene are designated $o_2(x_i, y_i, \theta_i)$. For each value of θ_i, each matrix is Fourier transformed along x_i and imaged along y_i. The 3-D matrix obtained is designated $o_3(u, v, \theta_i)$. Finally, from the entire 3-D matrix we select only the 2-D matrix with all the values that satisfy the equation $\theta_i = au$.

Next we show that, if a is chosen to be $a = -1/(2f)$, $h(u, v)$ is equal to the complex amplitude on the output plane of the equivalent coherent system, shown in Fig. 2(b). It should be emphasized that this coherent system is only the equivalent optical system for the expression in relation (6), and we depict it in Fig. 2(b) only to clarify the equivalent model. The complex amplitude is examined at the back focal plane of a convex cylindrical lens (horizontally focusing) when a plane wave is reflected from the 3-D object $o_1(x, y, z)$ located at the back focal plane and is perfectly imaged along the vertical axis. For a single infinitesimal element of the size $(\Delta x, \Delta y, \Delta z)$ from the entire object with an amplitude of $o_1(x', y', z')$, the complex amplitude at the plane (u, v) is[11,12]

$$g_1(u, v) = Ao_1(x', y', z')\delta(v - y) \times \exp\left[\frac{-i2\pi}{\lambda}\left(\frac{ux}{f} - \frac{u^2z}{2f^2}\right)\right]\Delta x\Delta y\Delta z, \quad (7)$$

where A is a constant. Summation over the contributions from all the points of the 3-D object yields the following complex amplitude:

$$g(u, v) = A \int\int\int o_1(x, y, z)\delta(v - y) \times \exp\left[\frac{-i2\pi}{\lambda}\left(\frac{ux}{f} - \frac{u^2 z}{2f^2}\right)\right] \mathrm{d}x\mathrm{d}y\mathrm{d}z. \quad (8)$$

Comparing Eqs. (8) and (6), we see indeed that substituting $a = -1/(2f)$ into Eq. (6) yields an expression similar to the one given in Eq. (8). The only difference is that $o_1(x, y, z)$ in Eq. (8) represents a complex amplitude, whereas in Eq. (6) it represents an intensity. As the intensity of the reconstructed object from $h(u, v)$ is proportional to $|o_1(x, y, z)|^2$, its gray-tone distribution is expected to be deformed compared with the gray-tone map of the original object. However, we can compensate for this deformation by computing the square root of the grabbed pictures in the recording stage. In both functions $h(u, v)$ and $g(u, v)$ the object's 3-D structure is preserved in a holographic manner. This means that the light diffracted from the hologram is focused into various transverse planes along the propagation axis according to the object's 3-D structure.

Parameter a can in fact take any arbitrary real value, not just the value $-1/(2f)$. In that case, after integration variable z is changed to $z' = -2faz$, Eq. (6) becomes

$$h(u, v) \propto \int\int\int o_1\left(x, y, \frac{-z'}{2af}\right)\delta(v - y) \times \exp\left[\frac{-i2\pi}{\lambda}\left(\frac{ux}{f} - \frac{u^2 z'}{2f^2}\right)\right] \mathrm{d}x\mathrm{d}y\mathrm{d}z'. \quad (9)$$

Relation (9) also has the form of Eq. (8) but with the change that the hologram obtained describes the same object on a different scale along its longitudinal dimension z. We conclude that by our choice of parameter a we can control the longitudinal magnification of the reconstructed image, as we show below.

Equation (8) represents a complex wave front, which usually should be interfered with a reference wave to be recorded. In the case of wave interference the intensity of the resultant interference pattern keeps the original complex wave front in one of four separable terms.[6] However, in our case the complex wave-front distribution is recorded into computer memory in the form of Eq. (6) [or relation (9)] without any interference experiment and actually without the need to illuminate the object with coherent laser light. Because the expression in Eq. (6) describes the equivalent of a wave-front distribution, it contains 3-D holographic information on the original objects, which can be retrieved as described in what follows.

As we mentioned above, the hologram values are stored in computer memory in the form of the complex function $h(u, v)$. To reconstruct the image from the hologram, the computer should modulate some transparency medium with the hologram values. If the transparency cannot be modulated directly with complex values, one of many well-known coding methods for CGHs[13] might be used. The spatial light modulator (SLM) that we use in this study can modulate the intensity of light with continuous gray tones. Therefore, complex function $h(u, v)$ is coded into a positive real transparency as follows,

$$h_r(u, v) = 0.5\left(1 + \mathrm{Re}\left\{h(u, v) \times \exp\left[\frac{i2\pi}{\lambda f}(\mathrm{d}_x u + \mathrm{d}_y v)\right]\right\}\right), \quad (10)$$

where $(\mathrm{d}_x, \mathrm{d}_y)$ is the new origin point of the reconstruction space and $|h(u, v)|$ is normalized at 0–1.

The holographic reconstruction setup is shown in the lower part of Fig. 1. To get the output image with the same orientation as the object, we display the 180°-rotated hologram $h(-u, -v)$ on the SLM. Then the SLM is illuminated by a plane wave, which propagates through the SLM and the two cylindrical lenses with two orthogonal axes. Through lens L_u, a 1-D FT of $h(-u, -v)$ along u is obtained at the back focal plane along x_o. Lens L_v images the distribution along the v axis on the y_o axis. This optical setup is identical to the equivalent coherent system shown in Fig. 2(b), and therefore the real image of the original 3-D object is reconstructed in the vicinity of the back focal plane of cylindrical lens L_u.

To calculate the magnification of the image along each axis we consider the equivalent optical process on object and on image planes. Based on Eq. (6) together with the operation of lens L_u, the effective

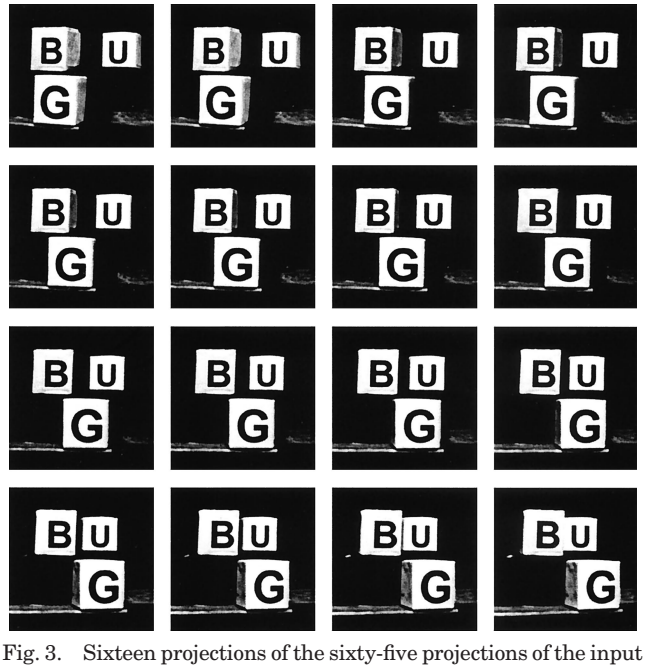

Fig. 3. Sixteen projections of the sixty-five projections of the input scene taken by the camera from various viewpoints.

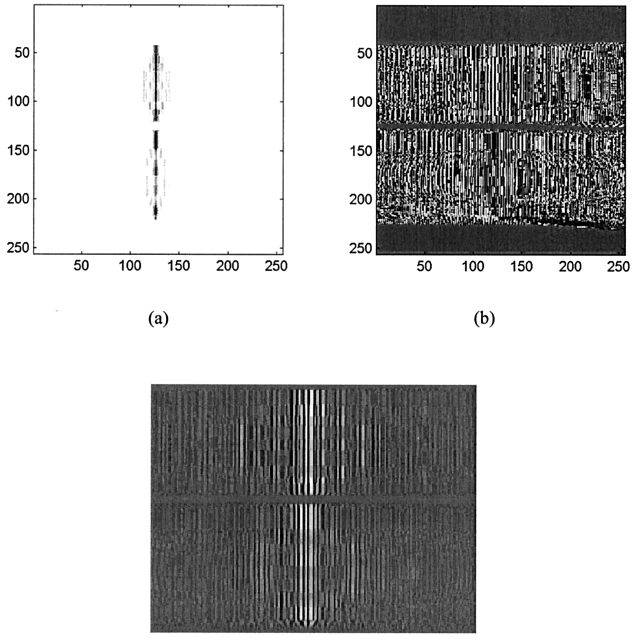

Fig. 4. (a) Magnitude (the maximum value is darkest) and (b) phase angle (π is white and $-\pi$ is black) of the hologram recorded and computed in the experiment. (c) Central part of the CGH, computed by Eq. (10) from the complex function shown in (a) and (b).

system from plane (x, y) to the output plane, along the horizontal axis, is similar to a 4-f system.[14] Therefore the overall horizontal magnification is identical to 1. In the vertical axis the object is imaged twice from plane (x, y) to output plane (x_o, y_o), and therefore the magnification is also equal to 1. On the longitudinal axis the situation is a bit more complicated. Looking at Eq. (6) and the Fourier lens L_u, we see a telescopic system but with two different lenses. From Eq. (6) the effective focal length of the first lens is $f_1 = \sqrt{f/(2|a|)}$. The focal length of reconstructing lens L_u is $f_2 = f$. Using the well-known result that the longitudinal magnification of a telescopic system[14] is $(f_2/f_1)^2$, we find the longitudinal magnification in our case to be $2f|a|$. Note that with parameter a one can control the image's longitudinal magnification independently of the transverse magnification.

3. Experimental Results

In our experiment the recording was carried out by the system shown in the upper part of Fig. 1 and the reconstruction was demonstrated first by a computer simulation of the system shown in the lower part of Fig. 1 and then by an optical experiment. The scene observed contains three cubes of size 5 cm × 5 cm × 5 cm located at different distances from the camera. We show in Fig. 3 16 examples selected from 65 scene viewpoints taken by the camera. Each projection contains 256 × 256 pixels. Figure 3 shows the scene observed by the CCD from a distance of 77 cm. The

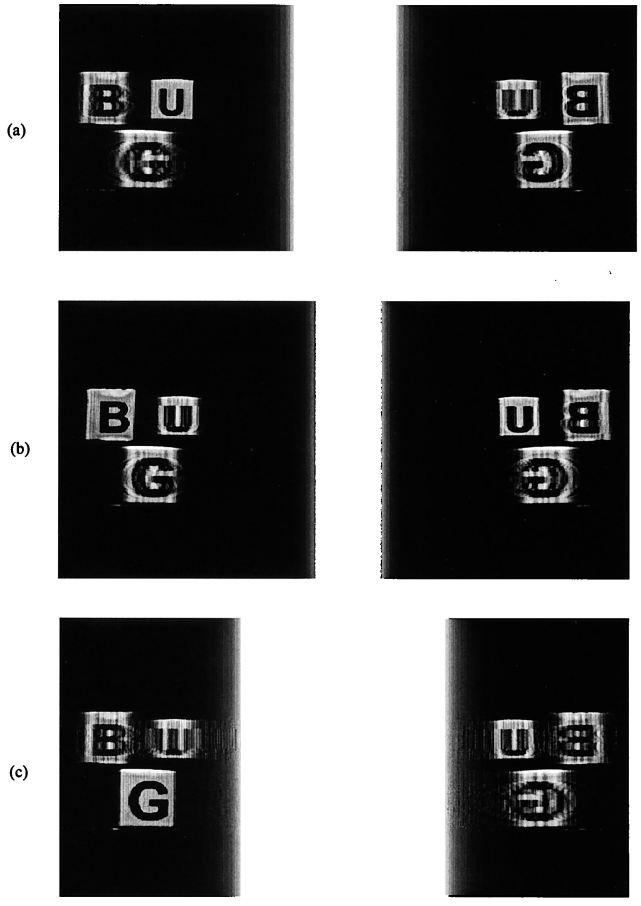

Fig. 5. Simulation results from the hologram shown in Fig. 4(c) at the vicinity of the back focal point of lens L_u for three transverse planes at (a) $z_o = -9f$, (b) $z_o = 6f$, (c) $z_o = 25f$.

angular range is ±16° from the CCD axis to the z axis, and the angular increment between every two successive projections is 0.5°.

The hologram was computed from the set of the 65 projections according to the procedure described above. Explicitly, for each picture, every row in every projection matrix was Fourier transformed. From the entire 3-D matrix obtained, we picked only the 2-D matrix placed on the diagonal plane expressed by the equation $\theta_i = au$. The magnitude and the phase angle of the computed 256 × 256-pixel complex function $h(u, v)$ are shown in Figs. 4(a) and 4(b), respectively. The central part of the CGH computed according to Eq. (10) is depicted in Fig. 4(c). The total size of the CGH is 800 pixels on the horizontal axis and 256 pixels on the vertical axis.

The reconstruction results from the hologram obtained from the computer simulation are depicted in Fig. 5. We obtained these results by calculating the diffraction behind the cylindrical lenses[15] for three values of z_o. Figure 5 shows the reconstructed intensity at three transverse planes along the optical axis. The figure shows the central three horizontal diffraction orders, whereas the zero order appears as the white area in the center of each part of Fig. 5; this area is thinner in Fig. 5(b) than in Figs. 5(a) and 5(c).

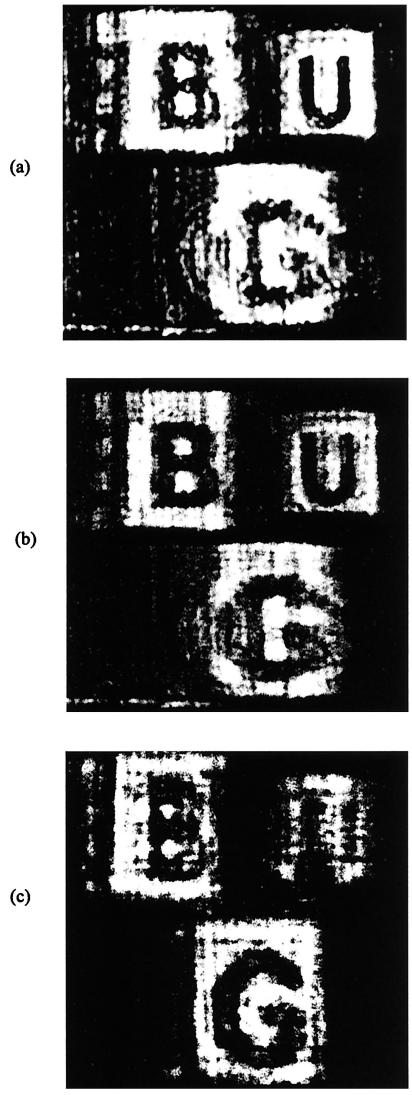

Fig. 6. Experimental results from the hologram shown in Fig. 4(c) at the vicinity of the back focal point of L_u for three transverse planes at (a) $z_o = -0.5$ cm, (b) $z_o = 2.5$ cm, (c) $z_o = 6$ cm.

At each transverse plane, in the left-hand diffraction order a different letter of a different cube is in focus; thus reconstruction of the 3-D objects is demonstrated.

In the optical experiment the CGH [part of which is shown in Fig. 4(c)] was displayed on a SLM (Central Research Laboratories, Model XGA1). Parameter a in this example was chosen to be $[\sin(32°)/3.5]$ cm^{-1}, where 32° is the angular range of the capturing camera and 3.5 cm is the width of the SLM located in the (u, v) plane. The reconstruction results in the region of the left-hand diffraction order are shown in Fig. 6 at three transverse planes along the optical axis. Evidently, the same effect in which every letter is in focus on a different transverse plane appears also in Fig. 6.

4. Conclusions

In conclusion, we have proposed and demonstrated a process of recording holograms of real-life 3-D objects without wave interference. There are two main differences between our method and previous techniques[16,17] for recording CGH's of 3-D objects. First, as we have shown, our hologram is a single hologram with properties similar to those of a hologram recorded optically by the interference of laser beams. Our hologram is neither a composite hologram nor a holographic stereogram as previously suggested.[16,17] Second, we deal with a real-life 3-D object recorded into computer memory, whereas others compute CGHs of artificial computer-generated objects. The last-named difference also distinguishes our method from the method of 3-D CGH suggested in Ref. 18.

This method is also different from the techniques for recording holographic stereograms and multiplex holograms[2–5] in two aspects. First, there is no need to interfere coherent beams in any stage of our process. The final CGH is obtained from the set of the object's projections purely by numerical computation. Second, our process is a true imitation of a particular holographic coherent system. Therefore the reconstructed image has features similar to those of an image coming from a coherently recorded hologram. This method might lead to development of a generally used holographic camera for outdoor photography.

This research was supported by the Israel Science Foundation.

References

1. D. Gabor, "A new microscope principle," Nature **161,** 777–779 (1948).
2. D. J. DeBitetto, "Holographic panoramic stereograms synthesized from white light recordings," Appl. Opt. **8,** 1740–1741 (1969).
3. P. Hariharan, *Optical Holography*, 2nd ed. (Cambridge U. Press, New York, 1996), Chap. 8, p. 139.
4. H. J. Caulfield, *Handbook of Optical Holography* (Academic, New York, 1979), Chap. 5, p. 211.
5. J. W. Goodman, *Introduction to Fourier Optics*, 2nd ed. (McGraw-Hill, New York, 1996), Chap. 9, p. 326.
6. Ref. 4, Chap. 3, p. 139.
7. Ref. 5, Chap. 5, p. 108.
8. D. L. Marks and D. J. Brady, "Three-dimensional source reconstruction with a scanned pinhole camera," Opt. Lett. **23,** 820–822 (1998).
9. M. R. Fetterman, E. Tan, L. Ying, R. A. Stack, D. L. Marks, S. Feller, E. Cull, J. Sullivan, D. C. Munson, Jr., S. T. Thoroddsen, and D. J. Brady, "Tomographic imaging of foam," Opt. Express **7,** 186–197 (2000), http://www.opticsexpress.org.
10. J. Rosen, "Three-dimensional joint transform correlator," Appl. Opt. **37,** 7538–7544 (1998).
11. Ref. 5, Chap. 5, p. 104.
12. J. Rosen, B. Salik, A. Yariv, and H.-K. Liu, "Pseudo-nondiffracting slitlike beam and its analogy to the pseudo nondispersing pulse," Opt. Lett. **20,** 423–425 (1995).
13. O. Bryngdahl and F. Wyrowski, "Digital holography—computer-generated holograms," in *Progress in Optics*, E. Wolf, ed. (North-Holland, Amsterdam, 1990), Vol. **28,** pp. 1–86.
14. Ref. 5, Chap. 8, p. 273.
15. B. Salik, J. Rosen, and A. Yariv, "One-dimensional beam shaping," J. Opt. Soc. Am. A **12,** 1702–1706 (1995).
16. T. Yatagi, "Stereoscopic approach to 3-D display using

computer-generated holograms," Appl. Opt. **15,** 2722–2729 (1976).
17. L. P. Yaroslavskii and N. S. Merzlyakov, *Methods of Digital Holography* (Consultants Bureau, New York, 1980), Chap. 1, p. 87.
18. C. D. Cameron, D. A. Pain, M. Stanley, and C. W. Slinger, "Computational challenges of emerging novel true 3D holographic displays," in *Critical Technologies for the Future of Computing*, S. Bains and L. J. Irakliotis, eds., Proc SPIE **4109,** 129–140 (2000).